CASPER:
COOPER AUTOMATED SUBTERRANIAN PROBING AND EXCAVATING ROBOT

ME 494 – BIO INSPIRED ROBOTICS

AUTHORS – KHUSHANT KHURANA, LEUNG LAM, SOHAIB BHATTI
MAY 11th, 2023

CONTENTS

I. INTRODUCTION

Burrowing bots are a class of mobile robots that dig into soil for the purposes of exploration, search and rescue, surveillance, monitoring, excavation, and construction. As opposed to robots capable of swimming in water or flying in air, burrowing bots need high power strokes to push against the resistance of the soil and overcome the drag along its surface, which is of orders of magnitude higher than that of air and water. Especially for vertical digging, the reaction forces and vertical stress induced from the soil demand even higher torques which not only cause the bot to deviate from its planned trajectory but also change the internal structure of the soil causing further complications. In a nutshell, the difficulties of creating robots for subterranean settings are exacerbated by the challenges of operating in granular media such as the substrate is dense, the environment is unstructured, and physical models for sand and soils are complex.

Most researchers try to solve this challenge by designing robots that emulate the digging patterns of actual organisms. Doing so not only allows them to find the efficient leg geometries that make excavating possible but also adds to the research of digging techniques used in nature. For example, a burrowing bot named "Crabot", developed by Rusell for locating underground chemicals, uses external flapping fins with feathering on the return stroke to locomote in horizontal planes of motion. Another set of scientists - (Barenboim & Degani, 2020) - use "vibro impact" to replicate the motion of a snake by using springs and creating a propulsion mechanism for the bot to dig. As the spring oscillates, the moving mass alternates, ultimately pushing the robot deeper into the sand.

Besides propulsion mechanisms, researchers have also progressed to applications of liquidation which is used by worms to help them move through the soil. In the case of robots, their tip is used to fluidize the granular media and convert the solid-state material to a fluid – like state material, which consequently helps them dig faster and more efficiently.

As shown above, researchers have tried to simulate the movements and strategies of the organisms to help advance the field of burrowing in robotics. To do the same with its research, the team pursued to focus on the different leg geometries and analyze them under the categories of digging ability, digging speed, required input power, digging patterns, and the complexity of these geometries.

II. DESIGN METHODOLOGY

For CASPER, the team decided to focus on replicating the motion of a mole crab. These crabs burrow by rotating their back legs clockwise (see 4 in figure 1) to create a pulling action, and rotating their front legs clockwise (see 3,2,1 in figure 1) to push sand upwards and themselves downwards into the sand. The crabs body pitches back and forth from the posterior and anterior legs, moving out of the way of the sand that is being shoveled upwards and allowing the crab to progress downwards. A figure representing the direction of rotation is shown in figure 1.
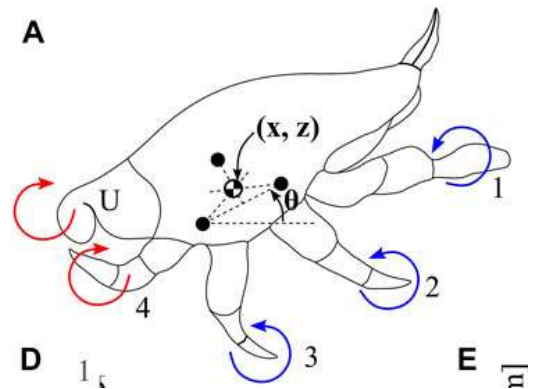

Figure 1. The anatomy of mole crab

While the front leg pair (labeled number 4) moves in a counterclockwise direction creating a pulling action, the other three pairs of legs work in a clockwise motion creating a pushing mechanism. The legs work together to shovel sand from underneath the mole crab and burrow itself in the sand. These pairs of legs are multi-jointed linkages and create power strokes in a specific pattern to help the animal burrow itself backwards into the sand.

Due to it being in its design stages, the team decided to take inspiration from Berkeley's EMBUR (Emerita Burrowing Robot) to design CASPER's body. A figure depicting EMBUR's design is shown in figure 2.
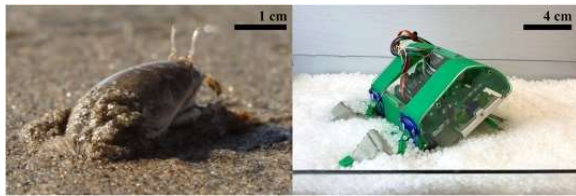

Figure 2 University of California, Berkeley's EMBUR Robot

EMBUR has two pairs of counterrotating legs driven by motors, emulating the motion of the posterior and anterior legs of the pacific mole crab. The path of these two legs is programmed by a piston like linkage. The researchers tracked the position of the legs and the robot using motion tracking cameras and saw how the motion of the legs corresponded to motion in the robot.

However, the researchers did not iterate on the design of the leg linkage, which could potentially yield better force transmission to the end effector, or a better trajectory. Even though their linkage works well in plastic pallets, they still fail to test out variations which can help the robot perform much better. Nevertheless, the paper does outline a great plan for building the robot's body which we can try replicate and improve rather than starting from scratch. This

would give the team more time to focus on the research topic at hand rather than spend time on fabrication of the robot.

Accordingly, CASPER compares two variations of leg geometry – Klann linkages and EMBUR's linkage geometry – iterating the dimensional parameters of each variation. The Klann linkage is a series of linkages that cause the end effector to follow a triangle shaped path. This paper focuses on the design of these linkages and the kinematics and dynamics associated with each one.

To do so, the team creates a test stand for each of these leg geometries to analyze and compare their behaviors. After a thorough evaluation of the benefits and drawbacks of each design is conducted and the team mounts the best leg design to the CASPER robot to analyze the performance while burrowing, rather than in place. A detailed fabrication of the two leg geometries is provided below.

A. KLANN GEOMETRY

Klann linkages, named after its inventor Matthias W. Klann, are a type of mechanical linkage system that is used for locomotion in robotics and other engineering applications. Designed to simulate the motion of a legged animal and act as a replacement to the traditional wheels, the linkage consists of a frame, crank, and four other linkages all connected by pivot joints. A figure demonstrating all these linkages is shown below.
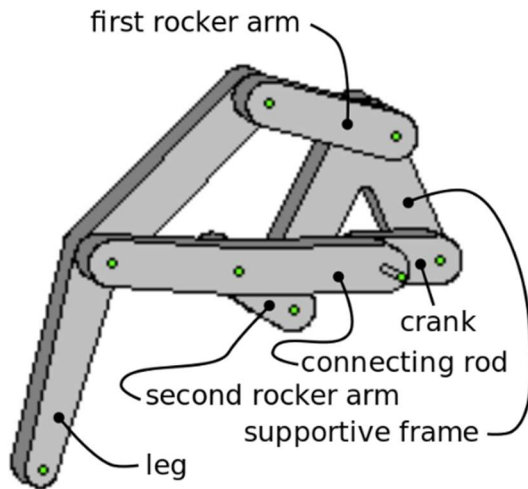
first rocker arm

crank

connecting rod

second rocker arm

supportive frame

leg

Figure 3 Computer aided model of Klann linkage representing its different components.

The length proportions of each of these linkages is optimally determined to allow for a smooth motion of the end effector – leg (as shown in figure 3) without having the linkages overlap to over constrain the motion. By having each linkage follow a partial circular motion relative to each other, the mechanism is able to convert rotational motion of the crank to the linear motion.

Speaking of crank, it acts as the mediator between the motor and the leg geometry. As it rotates 360 degrees, it transmits its rotational motion to the series of pivoting joints which in turn make the linkages rotate. For practical applications, Klann linkages serve as a great locomotion and digging models because of their ability to expand in a slanted direction for half of the rotation and retract in a symmetric way for other half of the rotation. By doing so, Klann linkages can jump over obstacles or dig into the ground without dragging their end effector – the leg.

Accordingly, the team decided to design a Klann geometry for CASPER and test its effectiveness

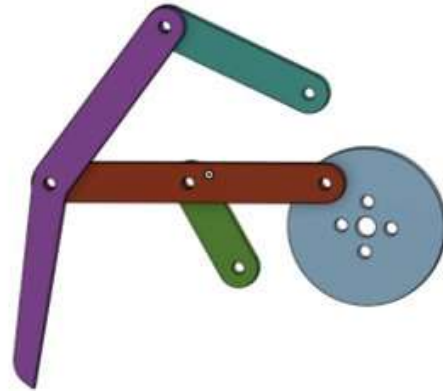in digging in rice. A computer aided model created for this is shown in figure 4.

Figure 4 Computer aided model of the Klann geometry for CASPER

The effective length of each of these linkages was determined using a modelling system created to simulate the kinematics which will be explained later. As said earlier, the light blue crank goes onto the stepper motor's hub forcing it rotate at the same frequency as the motor. In order to test the geometry, a test stand was also designed as shown in figure 5.
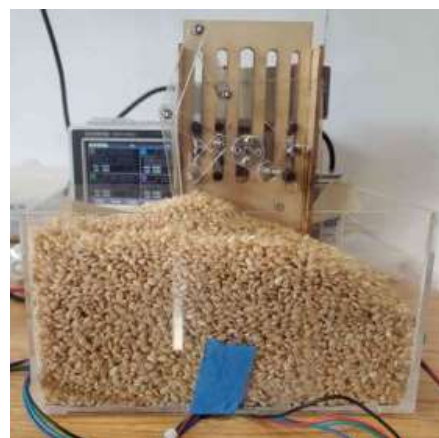

Figure 5 Test stand for CASPER's Klann geometry.

The test stand and the leg geometry were made from acrylic. Moreover, rice was used as the granular

media because of its small pellets. Since this was its first try in testing out the geometry, the team didn't want to use a medium with higher resistive forces which might hinder the motion of the linkage or require high torque motors.

B. EMBUR's LEG GEOMETRY

CASPER will use two pairs of counter-rotating legs: anterior and posterior. The anterior legs will simulate the pulling mechanism of mole crab (as done by pair 4 pictured in Figure 1) and the posterior legs will simulate the pushing mechanism (as done by pair 2).

The linkage design is similar to a piston, with a rod connected to the end of a driven crank using a pin joint. This rod is fed through a compliant linear slider which constrains the motion of the leg in the plane of the baseplate, but allows for all axis of rotation, as well as prismatic movement of the leg through the slot hole. This leg guide is made by sandwiching a cloth (light blue figure 6) between two 3mm washers (dark blue), then gluing the edges of the cloth to an acrylic mounting plate (yellow).
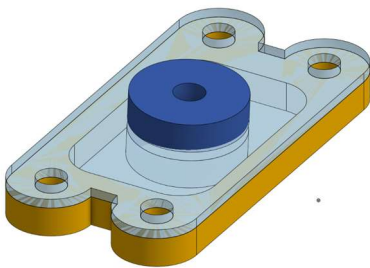

Figure 6. Leg guide assembly

This mounting plate is mounted onto a platform below the crank that touches the sand, such that the rod extends into the sand as it slides through the leg guide.
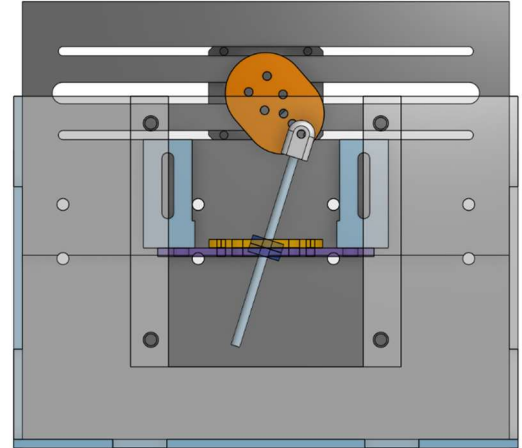

Figure 7.EMBUR leg geometry test stand with the crank (orange) and leg guide (yellow) mounted to the platform (purple)

The EMBUR leg geometry was mounted to a test stand that allowed the team to change several linkage parameters and see how these affect the path of the leg, as well as experimentally determine the force exerted by the leg. The crank on the test stand is driven by a 12V stepper motor controlled by a TMC 2208 stepper motor driver in its half stepping configuration, and an Arduino microcontroller. A stepper motor driver was chosen for the test stand because the position control of the motor makes it easy to set a very specific angular velocity for the motor so that the kinematics and dynamics of the system can be derived with the position of the motor as the variable q. The crank is connected to the motor by 4 M3 screws, which connect through the crank plate and into a motor mount, attached to the stepper motors 5mm d-shaft using a set screw. The radius at which the rod is pinned to the crank (r) can be changed as the crank plate has several holes at different radii from the driveshaft. The stepper motor is mounted horizontal slots of the back plate using M3 screws and washers; the slots allow the researchers to vary the position of the crank in the horizontal direction (a). The leg guide is mounted to a platform below the crank (purple in figure 7) which

3

has the digging medium directly below the platform. This platform is mounted to the back plate on the vertical slots of two 3d printed brackets (light blue in figure 7); these slots allow for the variation of the platform height (d). The length of the rod (l) unscrewing the rod from the hinge block (grey) and screwing in a rod of different length.

Tests were conducted varying the parameters – r,a,d, and l – on the test stand to evaluate how each parameter affects the kinematics or dynamics of the leg.

III. SIMULATIONS

To test out the design specifications chosen for CASPER, kinematic simulations were performed and mixed with design in order to come up with an efficient geometry. For both Klann and Embur's geometry, the team wanted the bot to follow a kidney bean shaped motion where it digs in a slanted way and retracts in a symmetric way. The reason behind this was that as the robot finishes its power stroke to dig, it should push the dug-out material to the rear without slicing its way through other areas. Accordingly, it was extremely important for the bot to move vertically up as it retracts, hence giving the kidney shaped curve in the bottom. The kinematic simulations done for CASPER are explained below.

A. Klann linkages

As explained before, it was extremely crucial to simulate the kinematics of the Klann geometry to ensure the legs wouldn't overlap with each other and the above-mentioned digging pattern can be achieved.

To simulate the geometry, a huge inspiration was taken from DIY walkers[1] and Paul Bourke's "Circle

Intersection Algorithm". Initially the team started to model all the constraints using trigonometric identities and physically applying constraints to each angular rotation. For example, the link connecting the crank and leg should stay between -45 to 45 degrees so that it does not interfere with other linkages. However, doing so not only made the analysis much harder due to the discontinuities in the rotation but also introduced many more tricky problems with coding the simulation.

Bourke's "Circle Intersection Algorithm" on the other hand uses the fact that crank can rotate 360 degrees to allow for the analysis to follow through get position of each link. To start the analysis, Bourke's suggests fixing two nodes around which the geometry can have constant rotation as shown in figure 8.
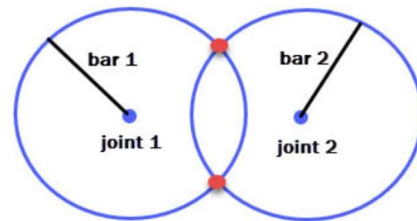

Figure 8.Graphical representation of the "Circle Intersection Algorithm"

Bourke's algorithm calculates the X and Y coordinates of the two red points where the circles intersect. Accordingly, the third joint that links the two bars will be one of these red points, whose choice remains on the design requirements. For the Klann geometry specifically, Bourke suggests starting with crank and a frame connection to find the third joint. Once the coordinates are known for third joint, the fourth joint can be positioned by tracing the circles of the third joint and the frame connection.

[1] References

After coding the simulation up, the Klann geometry (not to scale) derived is shown in figure 9.
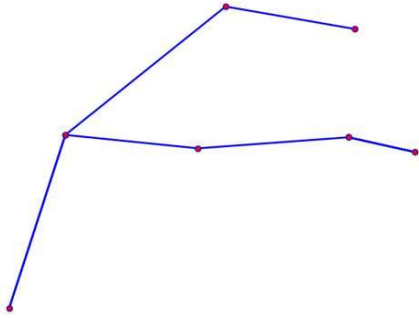

Figure 9. Simulated geometry for the Klann linkages using python

The simulation allows to enter the lengths of all the linkages, respective angles, and distances between the frame connections. Upon doing so, an actual working model of this can be visualized which was crucial in determining the lengths of the Klann geometry used for CASPER. Moreover, a graph depicting the simulated movement of the end effector – leg – of the geometry shown in figure 10. The final lengths of the linkages are depicted in Table 1.
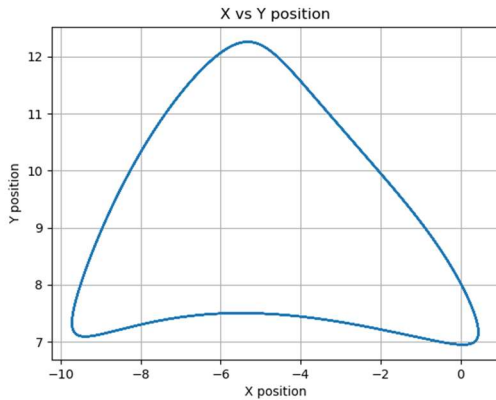

Figure 10.Theoretical motion of the end effector of the Klann geometry

Linkage color (as referenced in the cad model	Length (mm)
Red	70
Leg – Pink	50
Upper frame connection – Dark green	40
Lower frame connection – Light green	25
Crank distance (Pivot to pin joint)	15mm

Table 1: Final dimensions of the linkages used in Klann geometry
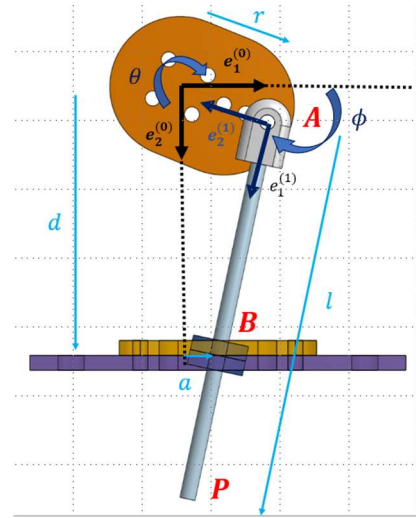
B. EMBUR's geometry

Figure 11.Diagram of the EMBUR leg geometry

The kinematics of the EMBUR linkage design can be described by the geometric constraint that the point B must be on the line between the hinge pin at A, and the end effector P. Firstly, the inertial frame $e^{(0)}$ is placed at the drive shaft of the motor. The position of pin A is described by $r_A = r(\cos(\theta)\hat{\imath} + \sin(\theta)\,\hat{\jmath})$. The point B is fixed in the inertial frame at the point $r_B = (a, d)$. To find the position of point P, a body fixed frame with its $e_1^{(1)}$ direction pointing in the direction AB is placed at A, such that the vector from A to P is always $(l, 0,0)$ in the body fixed frame $e^{(1)}$. To find the rotation matrix from frame 0 to frame 1 is a rotation about the $e_3^{(0)}$ axis by ϕ; ϕ is found using the dot product of AB and $e_1^{(0)}$

5

$$AB \cdot e_1^{(0)} = |AB| \cos(\phi)$$

$$\phi = \cos^{-1} \frac{\left(AB \cdot e_1^{(0)}\right)}{|AB|}$$

$$R_0^1 = R_{3,\phi}$$

From these coordinates, the position, velocity, acceleration and the angular acceleration of P can be determined.

$$r_p^{(0)} = r_A + R_0^1 * \begin{pmatrix} l \\ 0 \\ 0 \end{pmatrix}$$

$$v_p^{(0)} = \frac{\delta r_p^{(0)}}{\delta t} \quad a_p^{(0)} = \frac{\delta v_p^{(0)}}{\delta t} \quad \omega^{(0)} = \frac{\delta R_0^1}{\delta t}$$

The path of the end effector while varying each individual parameter is graphed below.
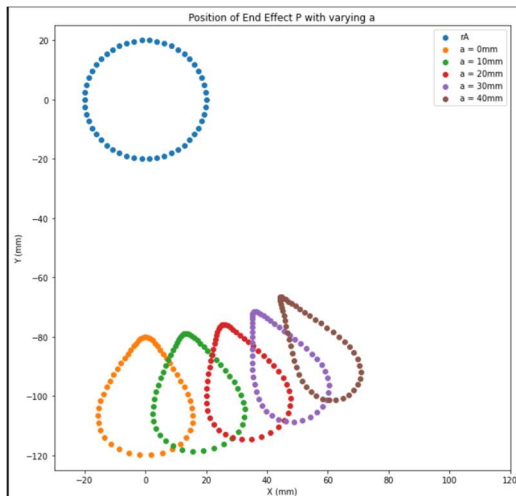

Figure 12. Postion of A (Blue) and position of end effector P with varying a's from 0-40mm. d=60mm, l=100mm, r=20mm
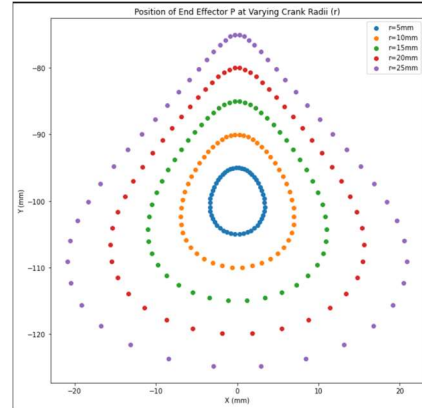

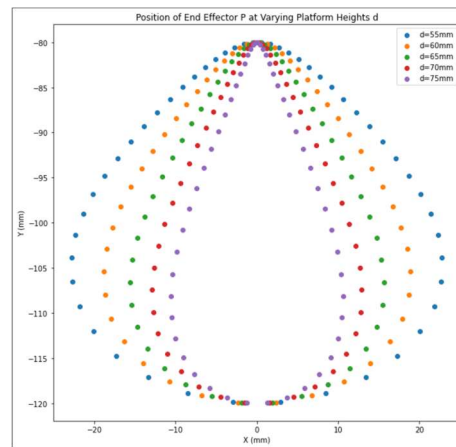Figure 13.Position of end effector P with varying crank radii (r), from 5mm-25mm. d=60mm, l=100mm, a=0mm

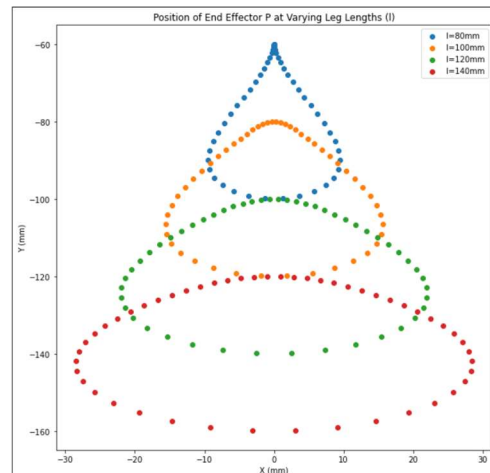Figure 14. Position of P with varying d from 55mm to 75mm. a =0mm, l=100mm, r=20mm

Figure 15.Position of P with varying l from 80-140mm. d=60mm, a=0mm, r=20mm

6

IV. EXPERIMENTAL DATA

After finishing the design for both geometries, testing w as conducted, and the results recorded are as follows. To ensure that the leg would work on its own before installing it on the chassis, the team elected to construct a test stand, where a motor, the leg, and a container for the medium (meant to represent the sand) can be installed. The leg stand was designed to allow vertical shifting of the motor and allowed the changing of leg parameters. The test stand was filled with short grain rice, a substance readily accessible, and emulates the shape of sand at a larger scale. To experimentally determine kinematics, the team used Tracker, which is software to conduct modelling through video analysis. Videos were taken of the legs in action which were then put into Tracker to track the position of the end effector.

a. Klann geometry

Since the tip of the end effector was hard to track visually since was submerged in the rice, the team decided to track the central point of the leg since it was always in line with the tip of the end effector. The locations of the specific point were recorded as a function of time and the following graphs were generated.
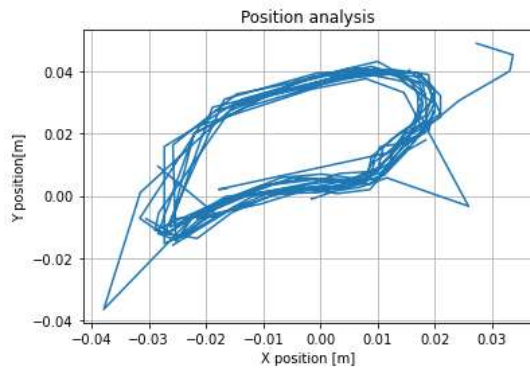

Figure 16. Experimental data for the end effector motion derived from Tracker.

The experimental data agrees with the simulation data where the tip of the end effector – leg – follows a kidney shaped motion where moves up as it retracts to prevent itself from dragging itself through the sand and dealing with unnecessary forces. This proved that the chosen lengths from the simulation were correct in not only allowing CASPER to follow the chosen digging pattern but also from overlapping with itself.

Since the position was derived as a function of time, the analysis was furthered by taking a numerical derivative and determine the velocity at each point. The graph generated is shown in figure 17.
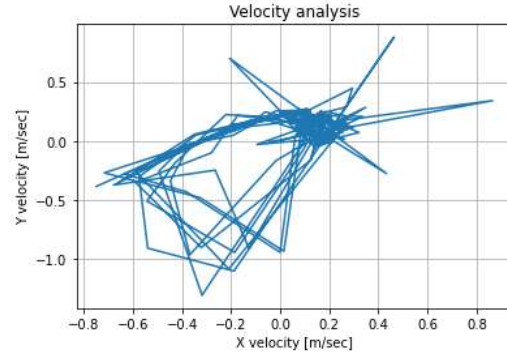

Figure 17. Velocity derived from discrete position points

Despite being extremely noisy, the velocity data does highlight some key points. Most important of which is that the top right corner is extremely chaotic. The reasoning is that is the point where CASPER's leg's velocity changes the most. As seen in figure 16, the end effector follows a very smooth motion without any quick maneuvers except the top which is resembled in the velocity graph.
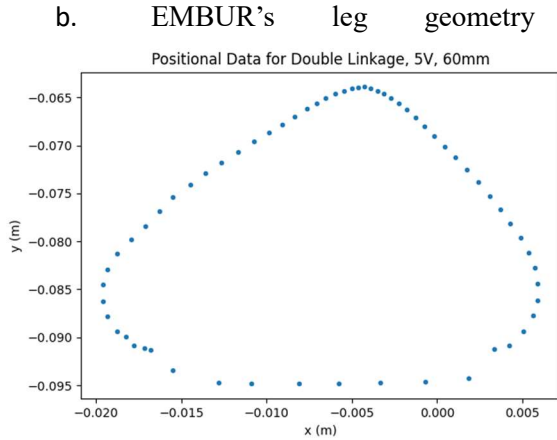
b. EMBUR's leg geometry

Figure 18. Experimental motion for the EMBUR geometry derived from Tracker

This set of experimental data agrees well with the theoretical predictions shown in figure 14, meaning the model is accurate. A similar kidney shape is developed by this leg geometry.

c. Overall observations

Based on observation, the EMBUR leg was able to dig the sand more deeply and emulated a burrowing motion more accurately. However, according to readings from the power supply used for the motor, this geometry also drew more current, corresponding to a higher power draw and work input.

V. CONCLUSION

Both designs were effective at what they were designed to do. The physical system's kinematics agreed with derived kinematics, which means the models are accurate for use in other evaluative quantities such as moments/forces or work input. Additionally, this also means that the design of the leg systems are accurate and thus are ready to be attached to the robot. Given they were both effective of burrowing through the medium present in the box, they should also be effective at helping the entire chassis burrow through the sand.

VI. FUTURE WORK

As CASPER's chassis has already been designed and manufactured, the tested leg geometries should be attached and tested. Even though the legs themselves were proven to be effective, they must be tested on the robot to ensure that the entire system is able to burrow through the ground.
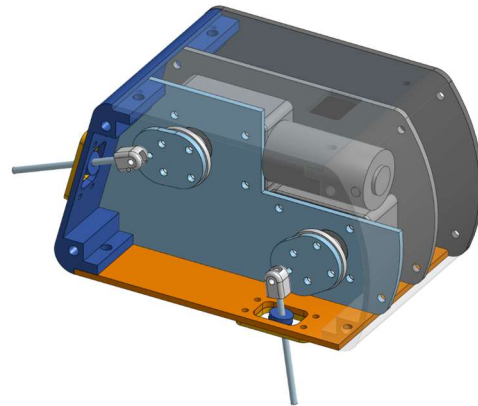

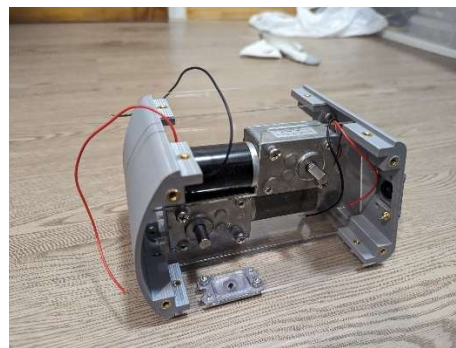*Figure 19. .Computer aided model of CASPER's body.*

Figure 20.CASPER robot without the top and side face plate, or legs attached.

The first iteration of CASPER was designed to be rapidly fabricated and modular to allow for quick iteration of the leg geometries. The front piece and

backpiece of the robot are 3D printed and heat-set inserts placed to connect to the rest of the robots chassis. Two worm screw dual-shaft motors are placed on top of each other and mounted to an acrylic centerplate on either side of the motors. These centerplates are slotted into a cutout in the center of the front and backpiece; if linkages were to be used in the future, holes can be laser-cut into the centerpiece for pin slots, making the design modular. Dual-shaft motors were used to eliminate the need for another external gear transmission to transmit the motor rotation to both sides of the robot. Worm screw motors are particularly good for application in digging because they are not back-drivable, and have a very high torque; since the robot does not need to dig quickly, and simply needs to dig with a lot of force, these characteristics make it ideal for use in CASPER. A motor hub is attached to each side of the drive shaft and a crank is mounted to each hub. A 3mm steel rod is attached at the end of each of these cranks using a m3 screw and a locknut, serving as a pivot joint. These are the legs of the robot. Each leg is fed through the same leg guide used in the paper above, mounted to the baseplate and backpiece of the robot. The acrylic baseplate and top plate are screwed into the heat-set inserts on the back and front piece. Then the sidewalls are screwed into the left and right faces of the back and front piece to complete the robot. In future work, the chosen legs will be mounted onto this robot and the burrowing capability of the robot will be tested.

VII.   REFERENCES

Barenboim, M., & Degani, A. (2020). Steerable Burrowing Robot: Design, Modeling and Experiments. *2020 IEEE International Conference on Robotics and Automation*.

Faulkes, Z., & Paul, D. (1997). Digging in sand crabs (Decapoda, Anomura, Hippoidea): interleg coordination. *Journal of Experimental Biology, 200*(4), 793–805.

Faulkes, Z., & Paul, D. H. (1998). Digging in sand crabs: coordination of joints in individual legs. *Journal of Experimental Biology, 201*(14), 2139–2149.

Russell, R. A. (2011). An agile burrowing robot for underground chemical source location. *Proceedings of Australasian Conference on Robotics and Automation*.

Russell, R. A. (2012). CRABOT: A Biomimetic Burrowing Robot Designed for Underground Chemical Source Location. *Advanced Robotics, 25*(1-2).

Treers, L. K., McInroe, B., Full, R. J., & Stuart, H. S. (2022). Mole crab-inspired vertical self-burrowing. *Frontiers in Robotics and AI*.

Trueman, E. R. (1970). The Mechanism of Burrowing of the Mole Crab, Emerita. *Journal of Experimental Biology*.